

RECEIVED: September 30, 2019

REVISED: December 4, 2019

ACCEPTED: December 25, 2019

PUBLISHED: February 6, 2020

21<sup>ST</sup> INTERNATIONAL WORKSHOP ON RADIATION IMAGING DETECTORS  
7–12 JULY 2019  
CRETE, GREECE

## PERCIVAL: possible applications in X-ray micro-tomography

G. Pinaroli,<sup>a,b,1</sup> G. Lautizi,<sup>c</sup> S. Donato,<sup>a,d</sup> L. Stebel,<sup>a</sup> G. Cautero,<sup>a</sup> D. Giuressi,<sup>a</sup> I. Gregori,<sup>a</sup>  
S. Dal Zilio,<sup>e</sup> R. Sergo,<sup>a</sup> M. Scarcia,<sup>a</sup> I. Cudin,<sup>a</sup> C.B. Wunderer,<sup>f</sup> J. Correa,<sup>f</sup> A. Marras,<sup>f</sup>  
S. Aplin,<sup>f</sup> B. Boitrelle,<sup>f,j</sup> F. Orsini,<sup>j</sup> P. Goettlicher,<sup>f</sup> M. Kuhn,<sup>f</sup> S. Lange,<sup>f</sup> M. Niemann,<sup>f</sup>  
I. Shevyakov,<sup>f</sup> M. Zimmer,<sup>f</sup> N. Guerrini,<sup>g</sup> B. Marsh,<sup>g</sup> I. Sedgwick,<sup>g</sup> A. Greer,<sup>h</sup> T. Nicholls,<sup>h</sup>  
U.K. Pedersen,<sup>h</sup> N. Tartoni,<sup>h</sup> H. Hyun,<sup>i</sup> K. Kim,<sup>i</sup> S. Rah,<sup>i</sup> H. Graafsma<sup>f,k</sup> and R.H. Menk<sup>a,l</sup>

<sup>a</sup>Elettra Sincrotrone Trieste, Trieste (TS), Italy

<sup>b</sup>University of UDINE, DIEGM, Udine (UD), Italy

<sup>c</sup>University of Trieste, Trieste (TS), Italy

<sup>d</sup>INFN section of Trieste, Trieste (TS), Italy

<sup>e</sup>Istituto Officina dei Materiali, CNR, Trieste (TS), Italy

<sup>f</sup>Deutsches Elektronen-Synchrotron (DESY), Hamburg, Germany

<sup>g</sup>Science & Technology Facilities (STFC), Didcot, U.K.

<sup>h</sup>Diamond Light Source (DLS), Didcot, U.K.

<sup>i</sup>Pohang Accelerator Lab (PAL), Pohang, South Korea

<sup>j</sup>Synchrotron SOLEIL, Saint Aubin, France

<sup>k</sup>Mid Sweden University, Sundsvall, Sweden

<sup>l</sup>Department of Medical Imaging, University of Saskatchewan, Saskatoon, SK S7N 5A2, Canada

E-mail: [pinaroli.giovanni@spes.uniud.it](mailto:pinaroli.giovanni@spes.uniud.it)

<sup>1</sup>Corresponding author.

**ABSTRACT:** X-ray computed micro-tomography ( $\mu$ CT) is one of the most advanced and common non-destructive techniques in the field of medical imaging and material science. It allows recreating virtual models (3D models), without destroying the original objects, by measuring three-dimensional X-ray attenuation coefficient maps of samples on the (sub) micrometer scale. The quality of the images obtained using  $\mu$ CT is strongly dependent on the performance of the associated X-ray detector i.e. to the acquisition of information of the X-ray beam traversing the patient/sample being precise and accurate. Detectors for  $\mu$ CT have to meet the requirements of the specific tomography procedure in which they are going to be used. In general, the key parameters are high spatial resolution, high dynamic range, uniformity of response, high contrast sensitivity, fast acquisition readout and support of high frame rates. At present the detection devices in commercial  $\mu$ CT scanners are dominated by charge-coupled devices (CCD), photodiode arrays, CMOS acquisition circuits and more recently by hybrid pixel detectors. Monolithic CMOS imaging sensors, which offer reduced pixel sizes and low electronic noise, are certainly excellent candidates for  $\mu$ CT and may be used for the development of novel high-resolution imaging applications. The uses of monolithic CMOS based detectors such as the PERCIVAL detector are being recently explored for synchrotron and FEL applications. PERCIVAL was developed to operate in synchrotron and FEL facilities in the soft X-ray regime from 250 eV to 1 keV and it could offer all the aforementioned technical requirements needed in  $\mu$ CT experiments. In order to adapt the system for a typical tomography application, a scintillator is required, to convert incoming X-ray radiation ( $\sim$  tens of KeV) into visible light which may be detected with high efficiency. Such a taper-based scintillator was developed and mounted in front of the sensitive area of the PERCIVAL imager. In this presentation we will report the setup of the detector system and preliminary results of first  $\mu$ CTs of reference objects, which were performed in the TomoLab at ELETTRA.

**KEYWORDS:** Computerized Tomography (CT) and Computed Radiography (CR); X-ray detectors; Image processing; Scintillators, scintillation and light emission processes (solid, gas and liquid scintillators)

---

## Contents

<b>1</b>	<b>Introduction</b>	<b>1</b>
<b>2</b>	<b>The PERCIVAL system</b>	<b>2</b>
<b>3</b>	<b>The scintillator</b>	<b>3</b>
<b>4</b>	<b><math>\mu</math>CT measurements</b>	<b>3</b>
4.1	$\mu$ CT of a sample	6
<b>5</b>	<b>Conclusions</b>	<b>7</b>

---

## 1 Introduction

X-ray micro-computed tomography ( $\mu$ CT) is a non-destructive imaging technique for the production of high-resolution three-dimensional (3D) images composed of two-dimensional (2D) trans-axial projections (180 or 360 mostly equi angular) of a target specimen. In general  $\mu$ CT equipment is composed of several components: an X-ray source, which might be a X-ray generator (cone beam) or a synchrotron radiation source (fan beam), filters and collimators, specimen movement stages and a suitable X-ray detector. This non-destructive imaging modality can produce 3D images and 2D maps with pixels even below  $1\ \mu\text{m}$ , thus giving its superior resolution to other techniques such as ultrasound and magnetic resonance imaging [1]. Consequently  $\mu$ CT is applied in a wide range of research fields, including materials science, medical, geophysical, environmental or paleontological studies, with increasing interest in dynamical imaging.  $\mu$ CT puts rather stringent requirements on the imaging detector. Just to mention a few it requires:

1. high dynamic range  $10^5 \sim 10^6$  with high linearity over the range
2. high spatial resolution ( $< 50\ \mu\text{m}$ )
3. high frame rates and fast temporal response
4. low afterglow of  $< 0.01\%$  within 100 ms after irradiation
5. low electronics noise compared to the associated quantum noise for all scan modes ( $\sigma_e < 0.5 \cdot \sigma_{\text{Poisson}}$ )
6. high detective quantum efficiency, ideally 100 %

Although single photon counting hybrid pixel detectors are excellent candidates as imaging detectors in this application it is mostly the pixel size that hinders their full exploitation in  $\mu$ CT. Thus indirect detection schemes based on scintillators coupled to CMOS imagers are still the most common technology for high resolution X-ray imaging. The PERCIVAL CMOS imager could in principle offer all the aforementioned technical requirements needed in  $\mu$ CT experiments. In order to adapt it a suitable scintillator possessing a high quantum efficiency is required.

## 2 The PERCIVAL system

PERCIVAL is a soft-X-ray detector under development as a collaboration between DESY, STFC, Elettra, DLS, PAL and SOLEIL in order to answer to the incoming needs from the unprecedented brilliance of 3<sup>rd</sup> generation storage rings as well as Free Electron Lasers (FELs) [2]. It is a 2D imager with small pixel pitch ( $27\ \mu\text{m}$ ) aimed at direct X-ray detection with high quantum efficiency in the 250-1000 eV (primary energy range), with an extended range down to  $<100\ \text{eV}$  and up to  $>2000\ \text{eV}$ . The PERCIVAL “P2M” system is the 2-million-pixel imager version, featuring a large uninterrupted imaging area of  $\approx 4 \times 4\ \text{cm}^2$ . An in-pixel circuitry is used to extend the dynamic range by modulating the pixel gain according to the impinging photon flux [3]. A system of three switches and capacitors is embedded in each pixel, able to change the charge-to-voltage transfer function of a pixel exposed to a high photon flux, thus avoiding its saturation and effectively increasing its dynamic range. This adaptive gain modulation (three gains) happens independently for each pixel and in real time allowing the detector to have at the same time a high gain for pixels exposed to a low photon flux and a coarser level of charge discrimination for pixels exposed to a high photon flux.

In figure 1, the scheme of the PERCIVAL system is reported.

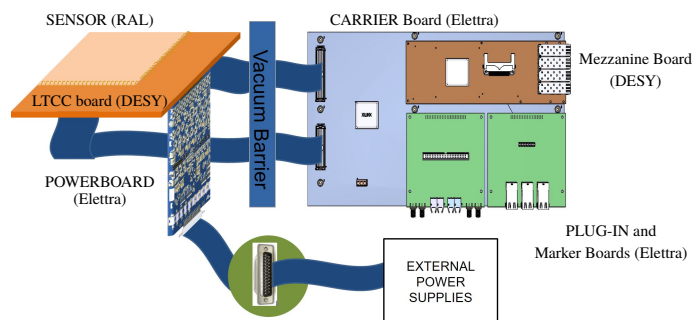


**Figure 1.** Scheme of the PERCIVAL system.

The main features of the detector are:

- Energy range, primary: 250 to 1000 eV, extended: 100 to 2000 eV
- QE over primary energy range: design goal  $> 85\%$  uniform over sensing area
- Frame rate up to 300 Hz
- Pixel size:  $27\ \mu\text{m}$
- Sensor Size: P2M version:  $1408 \times 1484$  pixels,  $4 \times 4\ \text{cm}^2$  uninterrupted
- Noise RMS  $< 15\ e^-$
- Full well  $3.5 \cdot 10^6\ e^-$ , resulting dynamic range:  $5 \cdot 10^4$  photons (at 250 eV)
- Exposure modes, FEL: all photons in  $< 300\ \text{fs}$ , synchrotron: quasi-continuous

Some P2M sensors in the Front Side Illuminated (FSI) configuration are being under tests and preliminary results have already been reported in [3, 4]. Moreover, the characterization of several smaller sized test prototypes, which had been built to evaluate the performance of the chosen architecture, has been reported in [5, 6]. In addition two wafers have been processed for soft X-ray compatibility and back side-illumination (BSI) compatible chips have been bonded to detector heads. First tests of these BSI devices are in progress.

### 3 The scintillator

One of the aforementioned Percival P2M FSI chips has been utilized during  $\mu$ -CT measurements at the TomoLab at Elettra in order to validate its applicability in such different application. Since the metal coverage is not complete the FSI is still sensitive to visible light. The quantum efficiency for green light has been evaluated for test structures with a similar pixel layout, which can be quoted between 10 and 20%. Of interest for  $\mu$ -CT application are the high dynamic range, low noise, large sensitive area in combination with a small pixel as well as its fast readout. Since Percival has been designed for soft X-rays below 1 keV, its 10  $\mu$ m sensitive Si layer does not provide sufficient quantum efficiency for the tenths of keV and more as required in standard tomography applications. Thus a scintillator screen is mandatory in order to convert the incoming high energy photons into visible light. Such scintillator screen has been custom developed at Elettra in collaboration with the Istituto Officina dei Materiali (IOM) of the Italian National Research Council (CNR). It is based on a composite of phosphor powder (P43) and optical glue. The lay-out of the scintillator is reported in figure 2 (left). The documented X-ray to visible-light yield of GADOX is in the range of 40–60 photons/keV [7], while the Aluminum thin film ( $\sim$  30 nm) was added to improve the efficiency of the scintillator and to mitigate the back scattered photons. In detail, a suspension has been prepared by mixing a suitable amount of P43 ( $\text{Gd}_2\text{O}_2\text{S:Tb}_3^+$  form USR Optonix Inc.) in Norland Optical Adhesive 74 (NOA 74) to achieve the correct viscosity for the following deposition procedure; the NOA glue shows high transmission in the visible spectrum region, low degassing in vacuum and the easy processing possibilities. The GADOX;NOA mix was deposited on the fiber taper and homogeneously distributed on the surface by a silk printing like method. A flood exposure system equipped with a UV lamp ( $\lambda = 250$  nm) has been employed to promote the cross linking of the optical glue, and a thermal treatment on a hot plate (120°C, 15 minutes) allowed the complete hardening. The deposition of the thin Al film has been performed in an e-gun based metal evaporator. The resulting scintillator screen has been fixed in front of the PERCIVAL imager utilizing a custom made aluminum holder (figure 2 (right)).

### 4 $\mu$ CT measurements

Measurements were performed at the Tomolab laboratory at Elettra <http://www.elettra.trieste.it/lightsources/labs-and-services/tomolab/tomolab.html>, [8]. The X-ray source is a sealed microfocus Hamamatsu X-ray tube (model L12161-07) with Tungsten target, that can operate at voltages between 40 and 150 KV at a maximum power of 75 W. It was used with the middle focal spot size, equivalent to 20  $\mu$ m. For the imaging experiments discussed here the tube voltage was set to 60 keV. Utilizing appropriate Al and Cu filters, the mean energy of the X-ray

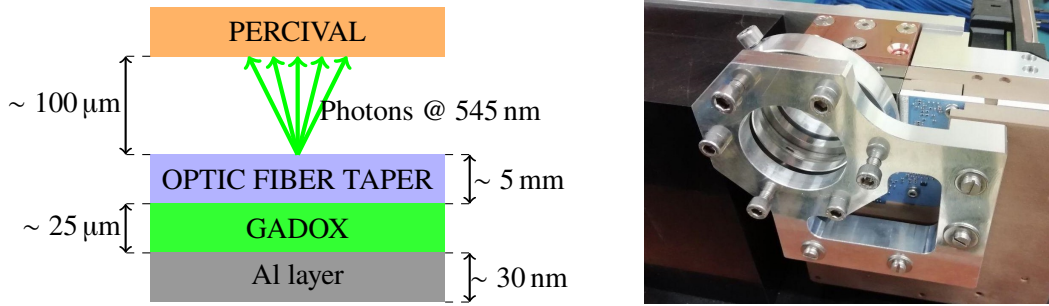


**Figure 2.** Stack layer diagram (left, layers size are not to scale) and the final detector system (right) upgraded with the aluminum scintillator holder which allows to adjust the device position (tilt and distance).

spectrum (figure 4 (left)) has been adjusted to approximately 23 keV with an energy spread of about 20 keV (FWHM). The source to detector distance was set to 1 m to guarantee uniform illumination (see figure 3). During the imaging and CT experiments the incident flux was adjusted such that no adaptive switching of the additional capacities would occurred. Therefore the overall dynamic in this configuration was governed by the fine bits only thus an equivalent of 12 bit. Since the sensor — intended for operation at  $-40\text{C}$  in a vacuum environment — was not cooled and had no temperature stabilization applied here the exposure time was set to 250 ms to keep the pedestal in the order of some tenths of ADUs. At first the linear response of the detector was measured using a uniform flat field illumination at different tube currents. For each tube current 100 flat images and dark frames, respectively, have been acquired. As depicted in figure 4 (right) the mean of the acquired ADUs (of  $1000 \times 1000$  pixels<sup>2</sup> and 100 frames) versus the tube current follows with high fidelity a linear behaviour ( $R = 0.99$ ). The error bars (sigma of the mean) are smaller than the symbols in this figure.

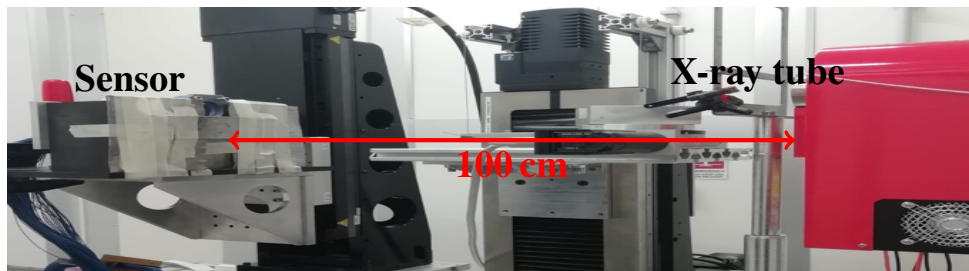


**Figure 3.** Measurement set-up at the TOMOLAB at Elettra.

The spatial resolution of the system comprising the sensor and the scintillator was estimated using the slanted edge method. The tube voltage was set to 40 kV and the current to  $300\ \mu\text{A}$ . A slightly tilted razor blade was placed in contact with the detector and then the Modulation Transfer Function was calculated using the Slanted Edge MTF plugin for ImageJ. The absolute MTF curve (in line pairs per millimeters, lp/mm) is shown in figure 5. At 10% of the MTF the spatial resolution obtained is 4.7 lp/mm corresponding to  $\sim 107\ \mu\text{m}$ . This large value, compared to the actual pixel size, is mostly dependent of the free air space between the optic fiber taper and the Percival sensor that contributes to the degradation of the spatial resolution. In addition to the MTF curve, we

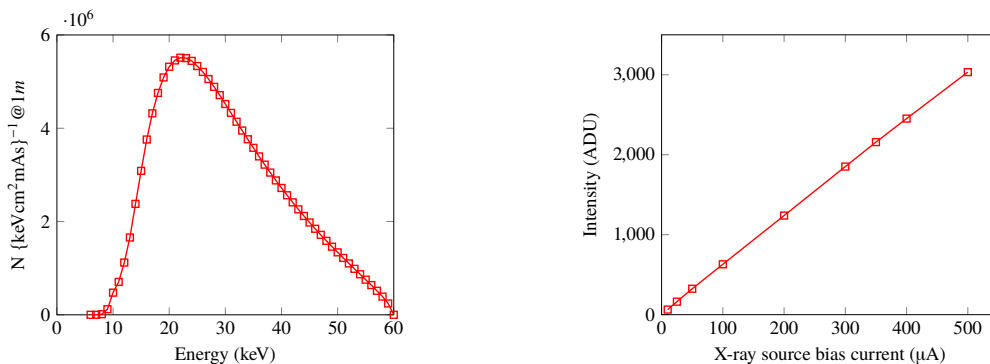


**Figure 4.** Spectrum of the X-ray source at TOMOLAB used during the beamtime (left) and the linear response of Percival under uniform illumination while the bias current of the source is increasing (right).

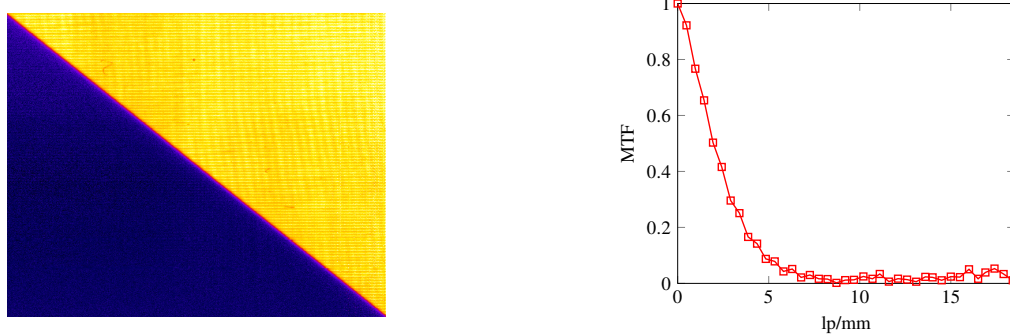


**Figure 5.** Flat-fielded Slanted Edge image for MTF calculation (left) and the resulting MTF curve for the sensor+scintillator system (right). Only flat and pedestal corrections have been applied to data.

measured the spatial resolution using a calibration bar-space pattern to obtain the Contrast Transfer Curve (CTF). The flat-fielded image is reported in figure 6 (left) while the corresponding grey-level profiles are shown in figure 6 (right). The contrast estimated at 4.5 lp/mm is equal to 5% while at 3 lp/mm is 17%. The measured resolution is in agreement with the MTF calculation.

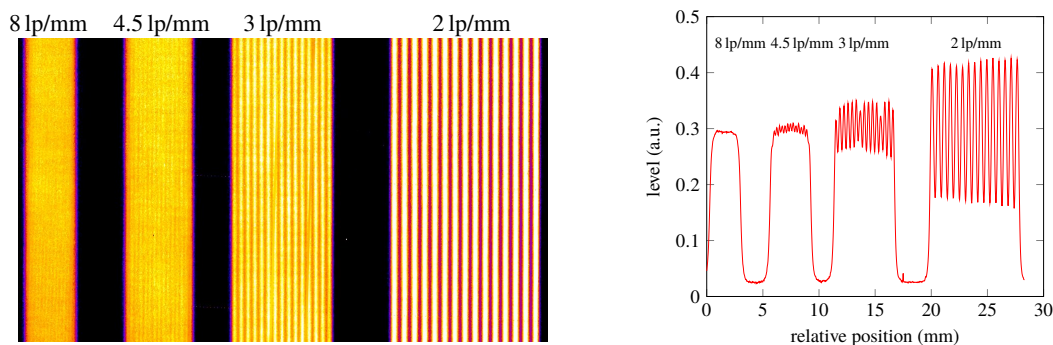


**Figure 6.** Funk lead bar pattern phantom (left) and the corresponding CTF plot (right). Only flat and pedestal corrections have been applied to data.

#### 4.1 $\mu$ CT of a sample

For the CT experiments a sample of biomedical significance has been selected. It is a matter of a single animal out of a larger group that had been used in a feasibility study of cell tracking ([9–11]). These animal experiments were carried out in accordance with the Canadian Council for Animal Care guidelines for animal trials, and the Animal Care Committee of the University of Saskatchewan approved the study. Moreover, the animal procedures were tailored in accordance with the European directive (86/609/CE - 1986). Permission to conduct the experiment was obtained in Canada and Italy. The ability to track cells in small-animal models of human disease is important because it gives the potential to improve our understanding of the processes of disease progression as well as our understanding of the therapeutic effects of interventions. In this study gold nanoparticles have been used as a permanent marker of implanted cell grafts. Using  $\mu$ CT the micrometric three-dimensional distribution of these marked cells could be displayed with penetration depth, high cell sensitivity and high spatial resolution in rodent models of human diseases. In principle the method allows quantification of cell numbers at any anatomical location over time in small animals.

In the case described here  $10^5$  U87 tumor cells, that are mimicking the most aggressive human brain cancer (glioblastoma multiforme) in a mouse model had been injected into the anterior right cerebra of 6 nude mice where they developed a clearly defined tumor after 7 days. At that time  $10^6$  gold nano particle labeled human mesenchymal stem cells (hMSCs) were injected into the right carotid artery of the animals. We demonstrated earlier ([9]) that hMSCs injected into the carotid artery of nude mice migrated towards and integrated into U87 glioma tumors present in the mice, thus could be used as a selective vehicle to transport diagnostic or therapeutic agents into the tumor. Twenty-four hours later the animals were sacrificed and preserved in a 10% buffered formalin solution for the post mortem CT acquisitions. For the CT experiments we used the head of one of these mice, which was placed in a sealed PMMA container at a source to sample distance of 25 cm (figure 7). Together with a sample to detector distance of 43 cm this results in a magnification of 4, thus in a virtual pixel size of  $15.7\ \mu\text{m}$ . The sample was rotated with constant angular speed, while the PERCIVAL detector was sampling the projections in continuous acquisition mode with an acquisition time of 250 ms per projection resulting in a total of 1440 equi angular projections over an angular arc of 360 degrees.

The overall acquisition time for an entire 3D data set was about 6 minutes. As an example one flat-field and dark field corrected projection is depicted in figure 7. No further image processing was applied to the projection data except the conventional flat fielding procedure.



**Figure 7.** Left: nude mouse head in PMMA container, right: one offset and gain corrected projection of the mouse head.



**Figure 8.** Orthogonal (axial, sagittal and coronal) slices of the mouse head.

A set of resulting orthogonal slice data is presented in figure 8, where the gold loaded hMSCs are indicated by the blue arrow in the axial (left), sagittal (middle) and coronal (right) planes. Owing the high dynamic of the reconstructed CT data permitted virtual volume segmentation and subsequently volume rendering of bone, brain tissue and gold nano particle loaded hMSCs which are depicted in the three panels of figure 9, respectively.

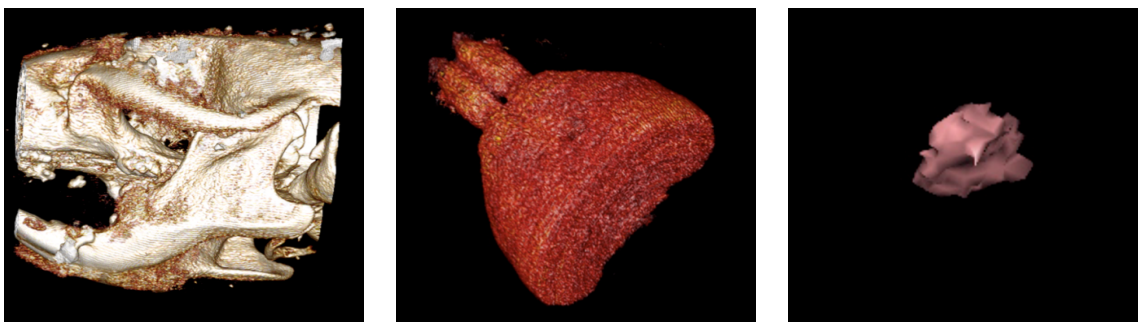


**Figure 9.** Segmented volume data.

As seen from the brain tissue rendering the olfactory bulb volume takes about 2% of the mouse brain by volume. Moreover, the hole in the anterior right cerebra, through which the U87 cells have been crafted, is clearly visible.

In the example shown in the right panel of figure 9 the hMSCs are incorporated into the tumor and occupy a volume of  $0.3 \text{ mm}^3$  that in combination of a cell volume of  $900 \mu\text{m}^3$  calculates to approximately 330,000 cells, which is about 33 % of the injected hMSCs.

## 5 Conclusions

The first application of the PERCIVAL imager in a  $\mu\text{CT}$  measurements, performed at the TomoLab laboratory at Elettra, has been reported. Results show that the detector possesses all the features to be a suitable candidate for these kind of applications when it is coupled to a scintillator screen. Several shortcomings of the set-up have been identified: firstly the measured spatial resolution is strongly limited by the gap between the sensitive area of the detector and the scintillator screen. However, the ease of fabrication process utilizing a composite of GADOX and optical glue opens definitively

the possibility of improving the device, by accurate thinning of the Gadox film, modulation of composition and type of the scintillator and eventually the “in progress” development of pixelated phosphors structures, allowing substantial increase of spatial resolution. Secondly the calibration routine of the detector plays a significant role on the measurements. Future efforts will therefore focus on thorough system calibration and the improvement of the scintillator coupling. This feasibility study revealed that in terms of its fast frame rate, the large field of view, its pixel size, the low noise and its high dynamic range scintillator coupled PERCIVAL FSI detectors are serious competitors to already existing systems.

## References

- [1] P. Müller, M. Schürmann and J. Guck, *The Theory of Diffraction Tomography*, [arXiv:1507.00466v3](https://arxiv.org/abs/1507.00466v3) [q-bio.QM].
- [2] H. Graafsma, *Requirements for and development of 2 dimensional X-ray detectors for the European X-ray Free Electron Laser in Hamburg*, 2009 *JINST* **4** P12011.
- [3] A. Marras et al., *Percival: A soft x-ray imager for synchrotron rings and free electron lasers*, in *Proceedings of the 13TH international conference on Synchrotron Radiation Instrumentation*, *AIP Conf. Proc.* **2054** (2019) 060060.
- [4] C.B. Wunderer et al, *The Percival 2-Megapixel monolithic active pixel imager*, 2019 *JINST* **14** C01006.
- [5] A. Kromova et al., *Report on recent results of the PERCIVAL Soft XRay Imager*, 2016 *JINST* **11** C11020.
- [6] J. Correa et al., *Characterisation of a PERCIVAL monolithic active pixel prototype using synchrotron radiation*, 2016 *JINST* **11** C02090.
- [7] H. Graafsma and T. Martin, *Detectors for synchrotron tomography*, in *Advanced Tomographic Methods in Materials Research and Engineering*, Oxford University Press, Oxford, U.K. (2008) [<https://www.oxfordscholarship.com/view/10.1093/acprof:oso/9780199213245.001.0001/acprof-9780199213245-chapter-10>].
- [8] L. Mancini et al., *TOMOLAB: the new Xray micro tomography facility at Elettra*, Elettra Highlights, Elettra, Trieste, Italy (2007).
- [9] R.H. Menk, E. Schültke, C. Hall, F. Arfelli, A. Astolfo, L. Rigon et al., *Gold nanoparticle labeling of cells is a sensitive method to investigate cell distribution and migration in animal models of human disease*, *Nanomed. Nanotechnol.* **7** (2011) 647.
- [10] A. Astolfo, E. Schültke, R.H. Menk, R.D. Kirch, B.H. Juurlink, C. Hall et al., *In vivo visualization of gold-loaded cells in mice using x-ray computed tomography*, *Nanomed. Nanotechnol.* **9** (2013) 284.
- [11] A. Astolfo, F. Arfelli, E. Schültke, S. James, L. Mancini and R.H. Menk, *A detailed study of gold-nanoparticle loaded cells using x-ray based techniques for cell-tracking applications with single-cell sensitivity*, *Nanoscale* **5** (2013) 3337.